Blind Channel Estimation in Full Duplex Systems: Identifiability Analysis, Bounds, and Estimators

Abbas Koohian, *Student Member, IEEE*, Hani Mehrpouyan, *Member, IEEE*, Ali A. Nasir, *Member, IEEE*, Salman Durrani, *Senior Member, IEEE*, Mohammad Azarbad, Steven D. Blostein, *Senior Member, IEEE*.

arXiv:1511.04794v2 [cs.IT] 18 Apr 2016

Abstract

We consider blind channel estimation in a single-input single-output full-duplex communication system, where both the self-interference and the communication channels need to be accurately estimated. In this context, blind estimators are attractive as they improve bandwidth efficiency, but they suffer from a phase ambiguity problem. In this paper, we first formally define and analyse this ambiguity and mathematically show that asymmetric constellations with respect to the origin can be used for blind channel estimation with no phase ambiguity. We present examples that involve shifted and rotated modulation sets. We propose an expectation maximization (EM) iterative estimator and a closed form minimum mean square error (MMSE) estimator for the asymmetric modulation sets. Since the non-data aided Cramér-Rao lower bound (CRLB) and the Bayesian CRLB (BCRLB) are intractable, we derive their data-aided CRLBs and BCRLBs to assess their performance. Simulations of shifted modulation sets show that the proposed estimators (i) approach the performance of their corresponding lower bounds, (ii) are robust to self-interference of the full-duplex signal, (iii) using rotated modulation sets reach data-aided estimation performance.

Index Terms

Blind channel estimation, identifiability analysis, full duplex communication, expectation maximization, minimum mean square error.

A preliminary version of this work was presented at 2015 IEEE ICC in London, UK [1]. Abbas Koohian and Salman Durrani are with Research School of Engineering, Australian National University, Canberra, Australia (email: {abbas.koohian, salman.durrani}@anu.edu.au). Hani Mehrpouyan is with the Department of Electrical and Computer Engineering, Boise State University, Idaho, USA (email: hani.mehr@ieee.org). Ali A. Nasir is with School of Electrical Engineering and Computer Science, National University of Science and Technology, Islamabad, Pakistan (email:ali.nasir@seecs.edu.pk). Mohammad Azarbad is with the Department of Mathematics, Statistics, and Computer Sciences, Tehran University, Tehran, Iran (email: m.azarbad@ut.ac.ir). Steven D. Blostein is with the Department of Electrical and Computer Engineering, Queen's University, Kingston, Ontario, Canada (email:steven.blostein@queensu.ca).

I. Introduction

Background: Full-duplex (FD) communication, allowing devices to transmit and receive in the same frequency band at the same time, is a promising technology to double the spectral efficiency of future wireless communication systems [2]–[4]. Recent studies have shown the performance improvement achievable with FD communication both theoretically [5]–[8] and experimentally [9]–[12]. The key challenge in realizing the benefits of FD communication is cancellation of the self-interference signal, which significantly corrupts the desired signal at the receiver [2]. There are two main approaches used in the literature to deal with this problem: (i) *passive* self-interference cancellation techniques, which attempt to isolate the transmit and receive antennas [13] and (ii) *active* self-interference cancellation techniques which use the knowledge of the self-interference signal to cancel the interference in the digital or the analog domain [9]. Although the power of the self-interfering signal is reduced by passive techniques, the residual power can still distort the desired signal significantly. Hence, it is important to have an accurate active cancellation stage.

Motivation: Active cancellation requires additional processing of the received signal compared to passive cancellation. For this reason and to have an effective active cancellation, accurate knowledge of the desired and the self-interference channels should be obtained [3], [9], [14]. The approach commonly used in the literature is to use pilots and to silence the transmitting node while estimating the self-interference channel, i.e., self-calibration. Once the self-interference channel is estimated, pilots are transmitted for the estimation of the communication channel [9]–[11]. A semi-blind approach for channel estimation in full duplex communication systems is proposed in [15], which still requires a few data-aided pilots to be transmitted. Data-aided piloting is a type of pilot-based estimation, where pilots symbols and data symbols are sent in different time slots. Hence, extra bandwidth is needed to estimate the channels [16]. Since FD communication requires two channels to be estimated, blind channel estimators with no data-aided piloting are more attractive as they can significantly improve bandwidth efficiency.

Blind channel estimation for conventional half-duplex (HD) communication systems has been thoroughly investigated in the literature. It is well-known that blind estimators can only estimate the channel up to a scaling factor and cannot recover the channel phases. The degree of this ambiguity can be determined using identifiability analysis, which determines whether a parameter can be uniquely estimated without any ambiguity [17]–[20]. Recently, blind estimators have been proposed for emerging systems such as amplify and forward two way relay networks (AF-TWRN) [21], [22] and interference limited networks [23], [24]. A shortcoming of recent research into blind estimators is a lack of parameter

identifiability analysis, which has inhibited achieving ambiguity-free blind channel estimation. Blind channel estimation in FD communication similarly requires a thorough identifiability analysis, with appropriate performance bounds and estimators.

Paper contributions: Blind channel estimation is investigated in a single-input single-output (SISO) full duplex (FD) communication system. The novel contributions include:

- *Identifiability analysis:* The condition for identifiability of channel parameters in FD communication systems is derived as Theorem 1, from which it follows that asymmetric modulation sets can be used for ambiguity-free channel estimation for communication systems involving two channels (e.g., FD communication, TWRN, and interference limited systems) without the need for data-aided piloting.
- *Proposed modulation sets*: Based on Theorem 1, we propose (i) a shifted modulation set constructed by applying a constant shift to symmetric modulation sets such as M-ary phase shift keying (M-PSK) and quadrature amplitude modulation (QAM), and (ii) a rotated modulation set constructed by applying an asymmetric rotation around the origin to symmetric modulation sets.
- *Proposed estimators:* We propose two estimators for simultaneous estimation of both interfering and communication channels using the new modulation sets: (i) a computationally efficient expectation maximization (EM) estimator to numerically obtain maximum likelihood (ML) channel parameter estimates, and (ii) a closed form minimum mean square error (MMSE) estimator to take advantage of known channel statistics, if available. The choice of MMSE estimator is motivated as follows: (i) prior information about the communication and the self-interference channels may be available [3], (ii) Bayesian estimators are known to minimize the Bayes risk cost function, i.e., average mean square error (MSE), which is an important performance metric for assessing the performance of estimators [25], and (iii) the MMSE estimator is closed form, which in turn means it does not suffer from convergence issues and does not require initialization as opposed to the EM estimator. Since the non-data aided Cramér-Rao lower bound (CRLB) or the Bayesian CRLB (BCRLB) are intractable, we derive the data-aided CRLB and the data-aided BCRLB to assess the performance of these estimators. We will also show that in contrast to the proposed estimators, direct pilot-based techniques either require a synchronized receiver and transmitter with orthogonal piloting or self-calibration.
- *Results:* Simulations show that proposed estimators (i) reach the performance of their corresponding lower variance bounds, (ii) are robust to an increasing self-interference power, (iii) can reach theperformance of corresponding data-aided bounds,when a rotated modulation set is used.

Notation: The following notation is used: bold face lower case letters, e.g., $\mathbf{x}$, are used for vectors. Bold face upper case capital letters, e.g., $\mathbf{X}$, are used for matrices. $\mathbf{I}_N$ represents the $N \times N$ identity matrix. $\mathrm{j} \triangleq \sqrt{-1}$, and the real and imaginary parts of a complex quantity are represented by $\Re\{\cdot\}$ and $\Im\{\cdot\}$, respectively. x^* and $|x|$ indicate scalar complex conjugate and the absolute value of complex number x, respectively. $\mathbb{E}[\cdot]$ is the expectation operator. $\det(\cdot)$, and $\mathbf{var}(\cdot)$ are the matrix transpose, the determinant, and variance operator, respectively. $\mathcal{O}(\cdot)$ represents the big $\mathcal{O}$ notation. $f(y)$ denotes the probability density function of random variable y. $\mathcal{CN}(\mu, \sigma^2)$ denotes a complex Gaussian distribution with mean μ and variance σ^2. $P(x)$ is the probability mass function (PMF) of discrete random variable x and $p(x = a)$ is the probability of a discrete random variable x taking the value a. $\mod$ is the modulo operator for which $a = b \mod c$ means $b = cd + a$ for some constant d.

II. System Model

We consider the channel estimation problem for a SISO FD communication system between two nodes a and b, as illustrated in Fig. 1. We assume channel reciprocity, which allows us to focus on the channel estimation problem at one node and apply the results to the other node [3]. Therefore, without loss of generality, we consider the estimation problem at node a only.

The received signal at node a is given by

$$\mathbf{y_a} = h_{aa}\mathbf{x}_a + h_{ba}\mathbf{x}_b + \mathbf{w_a}, \tag{1}$$

where $\mathbf{x_a} \triangleq [x_{a_1}, \cdots, x_{a_N}]$, $\mathbf{x_b} \triangleq [x_{b_1}, \cdots, x_{b_N}]$ are the $N \times 1$ vectors of transmitted symbols from node a and node b, respectively, $\mathbf{y_a} \triangleq [y_{a_1}, \cdots, y_{a_N}]$ is the $N \times 1$ vector of observations, $\mathbf{w_a}$ is the noise vector, which is modeled by N Gaussian independent elements, i.e., $\mathbf{w_a} \sim \mathcal{CN}(\mathbf{0}, \sigma^2\mathbf{I}_N)$, and h_{aa}, h_{ba} are the interference and communication channel gains, respectively. In this paper, we focus on the analysis under flat fading channels. The consideration of frequency selective channels makes the analysis more complicated but does not change the main results. Hence, it is not considered in this paper. Finally, we assume that the transmitted symbols are all equiprobable and drawn from modulation set $\mathcal{A} = \{x_1, x_2, ..., x_M\}$.

III. Blind channel estimation

In this section, we first formulate the blind channel estimation problem for the SISO FD communication system. Based on this formulation, we present a theorem that serves as a general framework for testing and designing modulation sets for ambiguity-free channel estimation without data-aided piloting in FD communication system.

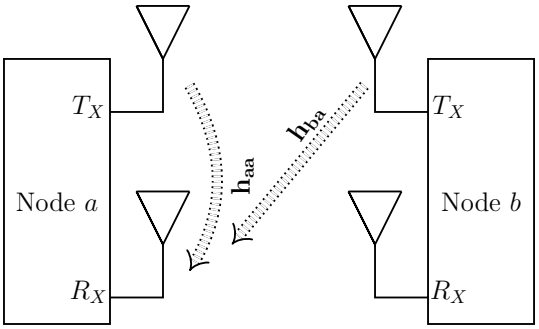

Fig. 1: Full duplex communication system with single transmit and receive antenna.

A. Problem Formulation

In formulating the problem, we make the following assumptions: (i) the transmitter is aware of its own signal, i.e., $\mathbf{x}_a$ is known at node a, which is a reasonable assumption [3], [9], (ii) the interference channel h_{aa}, and the communication channel h_{ba} are unknown parameters, (iii) the transmit symbol x_{b_i} from node b is an unknown discrete random variable with uniform distribution, and (iv) we observe N independent received symbols.

The parameter estimation problem requires the knowledge of the joint probability density function (PDF) of all observations. Given the system model in (1) and the above assumptions, the conditional PDF of a single observation is

$$f(y_{a_i}|x_{b_i}; h_{aa}, h_{ba}) = \frac{1}{\pi\sigma^2} \exp\left(\frac{-1}{\sigma^2}|y_{a_i} - h_{ba}x_{b_i} - h_{aa}x_{a_i}|^2\right), \tag{2}$$

where $i \in \mathcal{I} \triangleq \{1, \cdots, N\}$, y_{a_i} is the i^{th} received symbol, and x_{a_i} and x_{b_i} are the i^{th} transmitted symbols from node a and b, respectively. Note that y_{a_i} in (2) is a scalar because we start with the PDF of a single observation.

Then, the marginal PDF of a single observation is found by multiplying (2) by the uniform distribution $P(x_{b_i}) = \frac{1}{M}\mathbb{I}_{\{\mathcal{A}\}}(x_{b_i})$, and summing the results over all the possible values of x_{b_i}, where, $\mathbb{I}_{\{\mathcal{A}\}}(x) = 1$ if $x \in \mathcal{A}$ and 0 otherwise. Therefore, we have

$$\begin{aligned} f(y_{a_i}; h_{aa}, h_{ba}) &= \sum_{\forall x_{b_i}} f(y_{a_i}|x_{b_i}; h_{aa}, h_{ba})P(x_{b_i}) = \frac{1}{M\pi\sigma^2} \sum_{\forall x_{b_i}} \exp\left(\frac{-1}{\sigma^2}|y_{a_i} - h_{ba}x_{b_i} - h_{aa}x_{a_i}|^2\right)\mathbb{I}_{\{\mathcal{A}\}}(x_{b_i}) \\ &= \frac{1}{M\pi\sigma^2} \sum_{k=1}^{M} \exp\left(\frac{-1}{\sigma^2}|y_{a_i} - h_{ba}x_k - h_{aa}x_{a_i}|^2\right), \end{aligned} \tag{3}$$

where the last step follows from the fact that x_{b_i} is from the predefined modulation set $\mathcal{A}$. Finally, since we observe N independent observations, the joint PDF of all the observations is given by

$$f(\mathbf{y_a}; h_{aa}, h_{ba}) = \prod_{i=1}^{N} f(y_{a_i}) = \left(\frac{1}{M\pi\sigma^2}\right)^N \prod_{i=1}^{N}\sum_{k=1}^{M} \exp\left(\frac{-1}{\sigma^2}|y_{a_i} - h_{ba}x_k - h_{aa}x_{a_i}|^2\right), \tag{4}$$

and the blind channel estimation problem is defined as estimating h_{aa} and h_{ba} from (4). The PDF (4) will be used in Section V, in the optimization problem in the M-step of EM estimator, and will also be used to minimize the average MSE in the derivation of MMSE estimator.

B. Identifiability Framework

In this subsection, we present a theorem which serves as a general framework for parameter identifiability for blind channel estimation in FD communication systems. As a direct application, new modulation sets can be designed for ambiguity-free channel estimation without data-aided piloting.

We begin by presenting the following

Definition 1: [17, Chap:1] If $\mathbf{y}$ is a random variable distributed according to $f(\mathbf{y};\boldsymbol{\theta})$, then $\boldsymbol{\theta}$ is said to be unidentifiable on the basis of $\mathbf{y}$, if $\forall$ $\mathbf{y}$ there exists $\boldsymbol{\theta} \neq \boldsymbol{\theta}'$ for which $f(\mathbf{y};\boldsymbol{\theta}) = f(\mathbf{y};\boldsymbol{\theta}')$ and *if $\boldsymbol{\theta}$ is unidentifiable, then it is impossible for any estimator to uniquely determine the value of θ.*

For the sake of clarity and simplicity of analysis in this section we adopt the notation of Definition 1 and define $\boldsymbol{\theta} \triangleq [h_{aa}, h_{ba}]$. We also rewrite (4) accordingly as

$$f(\mathbf{y_a};\boldsymbol{\theta}) = \left(\frac{1}{M\pi\sigma^2}\right)^N \prod_{i=1}^{N}\sum_{k=1}^{M} \exp\left(\frac{-1}{\sigma^2}|y_{a_i} - \boldsymbol{\theta}(1)x_{a_i} - \boldsymbol{\theta}(2)x_k|^2\right), \tag{5}$$

where $\boldsymbol{\theta}(1)$ and $\boldsymbol{\theta}(2)$ represent the first and second elements of $\boldsymbol{\theta}$, respectively. Finally, the permutation function $\Pi(\cdot)$ is defined as a one-to-one and onto function on the index set of modulation set $\mathcal{A}$, i.e., $\mathcal{K} \triangleq \{1, 2, \cdots, M\}$. Consequently, if $x_k \in \mathcal{A}$, then, $x_{\Pi(k)} \in \mathcal{A}'$, $\forall k \in \mathcal{K}$, where $\mathcal{A}'$ is one possible permutation of original modulation set $\mathcal{A}$.

Lemma 1: $\boldsymbol{\theta}$ is not identifiable from (5), if and only if a permuted set $\mathcal{A}'$ exists, such that $\frac{x_k}{x_{\Pi(k)}}$ is a constant $\forall k \in \mathcal{K}$.

Proof: See Appendix A. ■

Theorem 1: Ambiguity-free blind channel estimation in FD communication is possible if and only if the modulation set is asymmetric with respect to the origin.

Proof: See Appendix B. ■

IV. Proposed modulation sets

To be power efficient, modulation constellations are conventionally designed to be symmetric around the origin. In this section, we apply Theorem 1 to construct (i) a shifted modulation set, by applying a constant shift to symmetric modulation sets such as M-PSK and QAM, and (ii) a rotated modulation set by applying an asymmetric rotation around the origin to symmetric modulation sets.

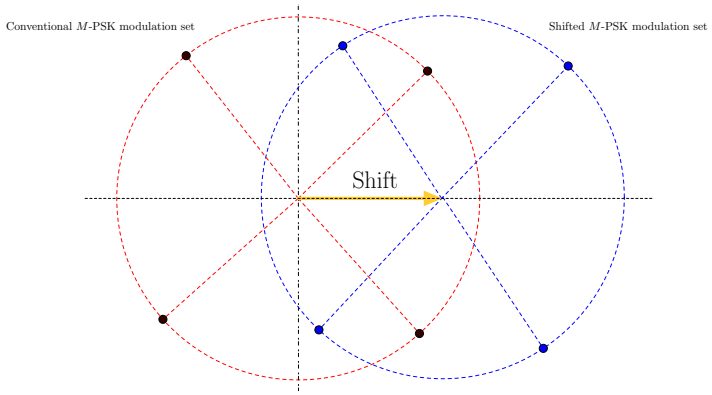

Fig. 2: Illustration of a shifted modulation set.

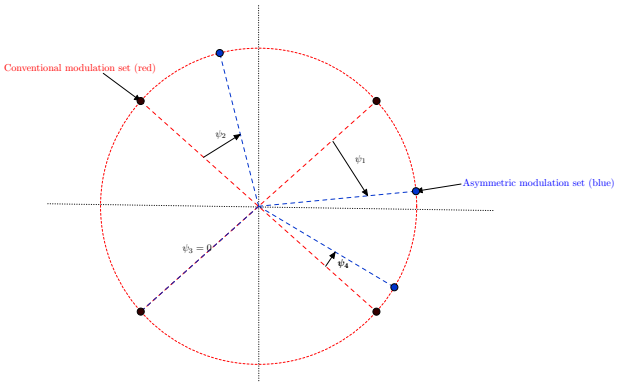

Fig. 3: Illustration of a rotated modulation set.

A. *Shifted modulation set*

A simple way to achieve constellation asymmetry would be to shift the constellation points of a symmetric constellation. According to Theorem 1, the resulting asymmetric modulation set can be used for ambiguity-free channel estimation. Without loss of generality, consider adding a real-valued constant α to each element of a given modulation set $\mathcal{A}$, then for $x_k \in \mathcal{A}$, shifted modulation set $\bar{\mathcal{A}}$ is defined as

$$\bar{\mathcal{A}} \triangleq \{\bar{x}_k \in \bar{\mathcal{A}} | \bar{x}_k = x_k + \alpha \quad \forall k \in \mathcal{K}\}. \tag{6}$$

For example, Fig. 2 shows the constellation diagram of a shifted M-PSK modulation constructed using (6).

Remark 1: Signals modulated by this new shifted M-PSK modulation set are of the form $A_m \cos(2\pi f_c t)\cos(\phi_m) - A_m \sin(2\pi f_c t)\sin(\phi_m)$, where A_m and ϕ_m are the phase and amplitude of mth element of shifted modulation set $\bar{\mathcal{A}}$, and f_c is the carrier frequency. In other words, they are embedded in the in-phase (I) and quadrature (Q) channels.

B. *Rotated modulation set*

Although the design of optimum asymmetric modulation sets is outside the scope of this work, we present an alternative to the shifted modulation set. An asymmetric modulation set may also be constructed from a given modulation set $\mathcal{A}$, by applying asymmetric rotation:

$$\bar{\mathcal{A}} \triangleq \{\bar{x}_k \in \bar{\mathcal{A}} | \bar{x}_k = x_k e^{\mathrm{j}\psi_k} \quad \psi_k \neq \psi'_k \quad \forall k, k' \in \mathcal{K}\}. \tag{7}$$

Fig. 3 is an illustration an M-PSK modulation constellation constructed using (7).

Remark 2: The proposed asymmetric modulation sets use extra resources to improve the quality of channel estimation. This extra resource can equivalently be used to send pilots in training-based estimation. For example, the power used to shift the modulation set can be used to send pilots tones at the carrier frequency. Assuming perfect synchronization between the transmitter and receiver, for the training-based system the received signal at node a is given by

$$\mathbf{y_a} = h_{aa}(\mathbf{x}_a + \mathbf{p}) + h_{ba}(\mathbf{x}_b + \mathbf{p}) + \mathbf{w_a}, \tag{8}$$

where $\mathbf{p}$ above is the constant pilot, which is equivalent to the constant shift in the shifted modulation set. (8) shows that even with the assumption of synchronized transmitter and receiver the unknown channel parameters (h_{aa} and h_{ba}) can not be estimated. To estimate the channel parameters using training-based techniques two different set of orthogonal pilots are needed. This is in contrast to the proposed estimation techniques, where no orthogonal pilot transmission is needed. Moreover, the proposed estimators are not constrained with the limiting assumption of synchronized transmitter and receiver.

Throughout the rest of the paper, we denote the new proposed modulation sets by $\bar{\mathcal{A}}$.

V. Proposed Estimators

In this section, we derive two estimators to obtain channel estimates in FD communication system with asymmetric modulation set $\bar{\mathcal{A}}$. We start the discussion on the estimators by presenting a computationally efficient EM estimator. We then derive closed form MMSE estimator to take advantage of the available prior information on the channel statistics. Appropriate performance bounds are then derived to assess the accuracy of the derived estimators. Finally in this section, we investigate the complexity of the estimators.

For the sake of notational brevity in what follows, we first define

$$\boldsymbol{\phi} \triangleq [\Re(h_{aa}), \Im(h_{aa}), \Re(h_{ba}), \Im(h_{ba})]. \tag{9}$$

A. EM Estimator

Problem Formulation: We can formulate the following ML problem:

$$[\Re(\hat{h}_{aa}), \Im(\hat{h}_{aa}), \Re(\hat{h}_{aa}), \Im(\hat{h}_{ba})] = \arg\max_{\boldsymbol{\phi}} (\ln f(\mathbf{y_a}; \boldsymbol{\phi})), \tag{10}$$

where $f(\mathbf{y_a};\boldsymbol{\phi})$ is given by (4). A common approach to solving the maximization problem in (10), is the well-known numerical EM algorithm [27], which is known to converge to a local maximum. The main steps of EM algorithm are[1]:

1) *Expectation step:* In the E-step, the expectation of the log-likelihood is taken over all the values of the hidden variable, conditioned on the vector of observations, and the nth estimate of $\boldsymbol{\phi}^{(n)}$, which is obtained from the M-step of the algorithm during nth iteration. In (1), the hidden variable is $\mathbf{x}_b$ and consequently, we need to evaluate $Q(\boldsymbol{\phi}|\boldsymbol{\phi}^{(n)}) \triangleq E_{\mathbf{x}_b|\mathbf{y}_a;\boldsymbol{\phi}^{(n)}}[\log f(\mathbf{y}_a,\mathbf{x}_b|\boldsymbol{\phi})]$.
2) *Maximization step:* In the M-step, the $Q(\boldsymbol{\phi}|\boldsymbol{\phi}^{(n)})$ function obtained from the E-step is maximized with respect to $\boldsymbol{\phi}$.
3) *Iterations:* We iterate between the E-step and M-step until convergence is achieved.

The equations needed for the E-step and M-step can be summarized in the propositions below.

Proposition 1: The E-step during nth iteration of the algorithm is given by

$$Q(\boldsymbol{\phi}|\boldsymbol{\phi}^{(n)}) = -N\ln(M\pi\sigma^2) - \frac{1}{\sigma^2}\sum_{i=1}^{N}\sum_{k=1}^{M} T_{k,i}^{(n)}|y_{a_i} - \hat{h}_{ba}^{(n)}\bar{x}_k - \hat{h}_{aa}^{(n)}\bar{x}_{a_i}|^2, \tag{11}$$

where $\bar{x}_k \in \bar{\mathcal{A}}\ \forall k \in \mathcal{K}$, $\bar{x}_{a_i} \in \bar{\mathcal{A}}\ \forall i \in \mathcal{I}$, $\hat{h}_{aa}^{(n)}$,$\hat{h}_{ba}^{(n)}$ are the estimates of the channels obtained from $\boldsymbol{\phi}^{(n)}$ during the nth iteration of the algorithm, and $T_{k,i}^{(n)}$ is defined as

$$T_{k,i}^{(n)} \triangleq \frac{\exp\left(\frac{-1}{\sigma^2}|y_{a_i} - \hat{h}_{ba}^{(n)}\bar{x}_k - \hat{h}_{aa}^{(n)}\bar{x}_{a_i}|^2\right)}{\sum_{\bar{k}=1}^{M}\exp\left(\frac{-1}{\sigma^2}|y_{a_i} - h_{ba}^{(n)}\bar{x}_{\bar{k}} - h_{aa}^{(n)}\bar{x}_{a_i}|^2\right)}, \tag{12}$$

where $\bar{x}_{\bar{k}} \in \bar{\mathcal{A}}\ \forall \bar{k} \in \mathcal{K}$

Proof: See Appendix C. ■

Proposition 2: The M-step during the nth iteration of the algorithm is given by

$$\boldsymbol{\phi}^{(n+1)} = \frac{1}{s_1 s_4 - s_2^2 - s_3^2}\begin{bmatrix} -s_2 v_3 - s_3 v_4 + s_4 v_1 \\ -s_2 v_4 + s_3 v_3 + s_4 v_2 \\ s_1 v_3 - s_2 v_1 + s_3 v_2 \\ s_1 v_4 - s_2 v_2 - s_3 v_1 \end{bmatrix}, \tag{13}$$

[1]The proposed EM algorithm for FD systems can be seen as a generalization of EM algorithms already existing in the literature to two simultaneously channels. The special case of half-duplex systems is obtained by setting the interference channel, i.e., h_{aa}, to zero.

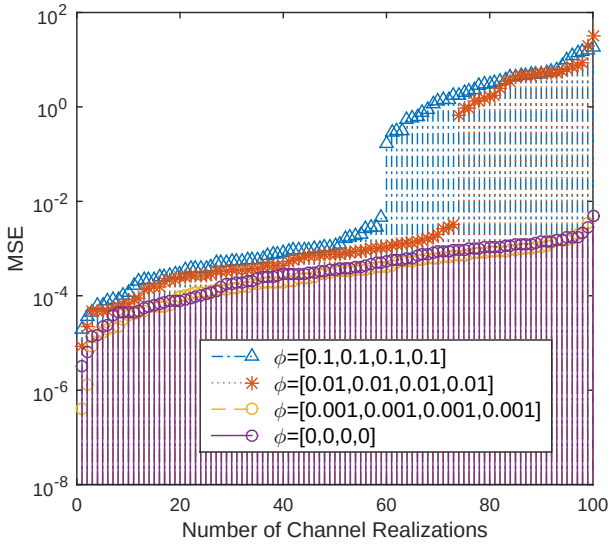

Fig. 4: The effect of different initialization on MSE for $N = 32$ observations at SNR = 20 dB.

where

$$s_1 \triangleq \sum_{i=1}^{N} |\bar{x}_{a_i}|^2,\ s_2 \triangleq \sum_{i=1}^{N}\sum_{k=1}^{M} T_{k,i}^{(n)} \Re(\bar{x}_{a_i}\bar{x}_k^*),\ s_3 \triangleq \sum_{i=1}^{N}\sum_{k=1}^{M} T_{k,i}^{(n)} \Im(\bar{x}_{a_i}\bar{x}_k^*),\ s_4 \triangleq \sum_{i=1}^{N}\sum_{k=1}^{M} T_{k,i}^{(n)} |\bar{x}_k|^2 \quad , \tag{14a}$$

$$v_1 \triangleq \sum_{i=1}^{N} \Re(\bar{x}_{a_i}^* y_i),\quad v_2 \triangleq \sum_{i=1}^{N} \Im(\bar{x}_{a_i}^* y_i),\quad v_3 \triangleq \sum_{i=1}^{N}\sum_{k=1}^{M} T_{k,i}^{(n)} \Re(y_i \bar{x}_k^*),\quad v_4 \triangleq \sum_{i=1}^{N}\sum_{k=1}^{M} T_{k,i}^{(n)} \Im(y_i \bar{x}_k^*). \tag{14b}$$

Proof: See Appendix C. ■

Remark 3: It is well-known that the EM algorithm is very sensitive to initialization [28]. Although different methods exist for EM initialization, generally they are not computationally efficient [28], [29]. Consequently, we rely on simple and empirical EM initialization. In Fig. 4, we plot sorted MSE for 100 different channel realizations at SNR$=20$ dB when binary phase shift keying (BPSK) modulation is used. To allow for a fair comparison, we initially generated 100 random realizations of the channels and used them to obtain the MSE performance of EM estimator for all four different initialization of $\boldsymbol{\phi}$. It is clear from the figure that as we deviate from zero at the initialization stage, the number of MSE outliers increases significantly. Increasing the number of outliers results in poorer performance for average MSE. Consequently, we initialize the EM algorithm by $\boldsymbol{\phi} = [0, 0, 0, 0]$.

B. MMSE Estimator

Problem Formulation: We first formulate the Bayesian channel estimation problem, which is different from ML channel estimation given by (10)*. The MMSE channel estimates* $\hat{h}_{aa}$ *and* $\hat{h}_{ba}$ *are given by*

$\mathbb{E}[h_{ba}|\mathbf{y_a}]$ *and* $\mathbb{E}[h_{ba}|\mathbf{y_a}]$*, respectively. It is well known that these estimates minimize the average MSE cost functions, i.e.,* $\mathbb{E}_{h_{aa}}[\mathbb{E}_{\hat{h}_{aa}}[|h_{aa}-\hat{h}_{aa}|^2]]$, $\mathbb{E}_{h_{ba}}[\mathbb{E}_{\hat{h}_{ba}}[|h_{ba}-\hat{h}_{ba}|^2]]$ [25].

We adopt the conventional assumption about the channels in FD communication system and assume the channel links between nodes a and b are modelled using small-scale Rayleigh fading. Thus, the complex fading coefficients of the self-interference channel, h_{aa}, and the communication channel, h_{ba}, are assumed to be circularly symmetric complex Gaussian (CSCG) random variables with zero mean and unit variance, i.e., $h_{aa}, h_{ba} \sim \mathcal{CN}(0,1)$ [3], [11], [14], [30].

Proposition 3: The MMSE estimators for the communication and self-interference channels are given by

$$\hat{h}_{ba} = \frac{-K\pi\sigma^4}{f(\mathbf{y_a})} \sum_{k_N=1}^{M} ... \sum_{k_1=1}^{M} \frac{\Upsilon^*}{|\Omega^*|^2} \exp\left(\frac{-1}{\sigma^2}\left(\Lambda - \frac{|\Upsilon|^2}{\Omega^*}\right)\right), \tag{15a}$$

$$\hat{h}_{aa} = \frac{-K\pi\sigma^4}{f(\mathbf{y_a})} \sum_{k_N=1}^{M} ... \sum_{k_1=1}^{M} \frac{\Upsilon_a^*}{\omega|\omega_a|^2} \exp\left(\frac{-1}{\sigma^2}\left(\Lambda_a - \frac{|\Upsilon_a|^2}{\Omega_a^*}\right)\right), \tag{15b}$$

where σ^2 is the noise variance, $K \triangleq (\frac{1}{\pi})(\frac{1}{M\pi\sigma^2})^N$, the joint PDF of all observations $f(\mathbf{y_a})$ is given by

$$f(\mathbf{y_a}) = \frac{K\pi\sigma^4}{\omega} \sum_{k_N=1}^{M} ... \sum_{k_1=1}^{M} \frac{1}{\Omega} \exp\left(-\frac{1}{\sigma^2}\left(\Lambda - \frac{|\Upsilon|^2}{\Omega^*}\right)\right). \tag{16}$$

Moreover, in (15a) and (16)

$$\Lambda \triangleq \sum_{i=1}^{N} |y_{a_i}|^2 - \frac{1}{\omega^*}\left|\sum_{i=1}^{N} y_{a_i}^* \bar{x}_{a_i}\right|^2, \tag{17a}$$

$$\Omega \triangleq \sigma^2 + \sum_{i=1}^{N} |\bar{x}_{k_i}|^2 - \frac{1}{\omega^*}\left|\sum_{i=1}^{N} \bar{x}_{a_i}\bar{x}_{k_i}^*\right|^2, \tag{17b}$$

$$\Upsilon \triangleq \frac{(\sum_{i=1}^{N} \bar{x}_{a_i}^* \bar{x}_{k_i})(\sum_{i=1}^{N} y_{a_i}^* \bar{x}_{a_i})}{\omega^*} - \sum_{i=1}^{N} y_{a_i}^* \bar{x}_{k_i}, \tag{17c}$$

$$\omega \triangleq \sigma^2 + \sum_{i=1}^{N} |\bar{x}_{a_i}|^2, \tag{17d}$$

and in (15b)

$$\Lambda_a \triangleq \sum_{i=1}^{N} |y_{a_i}|^2 - \frac{1}{\omega_a} \left| \sum_{i=1}^{N} y_{a_i}^* \bar{x}_{k_i} \right|^2, \tag{18a}$$

$$\Omega_a \triangleq \sigma^2 + \sum_{i=1}^{N} |\bar{x}_{a_i}|^2 - \frac{1}{\omega_a} \left| \sum_{i=1}^{N} \bar{x}_{k_i} \bar{x}_{a_i}^* \right|^2, \tag{18b}$$

$$\Upsilon_a \triangleq \frac{(\sum_{i=1}^{N} \bar{x}_{k_i}^* \bar{x}_{a_i})(\sum_{i=1}^{N} y_{a_k}^* \bar{x}_{k_i})}{\omega_a} - \sum_{i=1}^{N} y_{a_i}^* \bar{x}_{k_i}, \tag{18c}$$

$$\omega_a \triangleq \sigma^2 + \sum_{i=1}^{N} |\bar{x}_{k_i}|^2, \tag{18d}$$

where $k_i \in \mathcal{K}$, $\forall i \in \mathcal{I}$, $\bar{x}_{k_i}$ is the k_ith element of asymmetric modulation set $\bar{\mathcal{A}}$, and $\bar{x}_{a_i}$ is ith transmitted symbol from node a that has been modulated by the asymmetric modulation set $\bar{\mathcal{A}}$.

Proof: See Appendix D. ■

C. Performance Bounds

In blind channel estimation problems with asymmetric modulation sets, the actual data is not known. For this reason, non data-aided bounds can be considered as suitable performance benchmarks. However, these bounds cannot be derived in closed form [31]–[33]. Hence, we resort to the data-aided bounds. We first derive the data-aided CRLB for EM estimator and then use this bound to derive the data-aided BCRLB for Bayesian estimators. To allow for a fair comparison with the blind estimators using asymmetric modulation sets, the bounds are also derived for asymmetric modulation sets, i.e., the ith transmitted symbols $\bar{x}_{a_i}, \bar{x}_{b_i} \in \bar{\mathcal{A}}$.

1) Data-aided CRLB: The CRLB for data-aided estimation is used as a benchmark for the EM estimator and is presented in the proposition below.

Proposition 4: The *CRLB* for estimation of parameters of interest is

$$\mathbf{var}(\hat{\boldsymbol{\phi}}_l) \geq \left[\mathbf{I}^{-1}(\boldsymbol{\phi})\right]_{l,l}, \tag{19}$$

where in (19), $l \in \{1, 2, 3, 4\}$, $\mathbf{I}(\boldsymbol{\phi})$ is the 4×4 Fisher information matrix (*FIM*) with its elements given by

$$\mathbf{I}_{1,1} = \mathbf{I}_{2,2} = \frac{2}{\sigma^2} \sum_{i=1}^{N} |\bar{x}_{a_i}|^2. \qquad \mathbf{I}_{3,3} = \mathbf{I}_{4,4} = \frac{2}{\sigma^2} \sum_{i=1}^{N} |\bar{x}_{b_i}|^2, \tag{20a}$$

$$\mathbf{I}_{2,4} = \mathbf{I}_{4,2} = \mathbf{I}_{1,3} = \mathbf{I}_{3,1} = \frac{2}{\sigma^2} \sum_{i=1}^{N} \left(\Re\{\bar{x}_{a_i}\}\Re\{\bar{x}_{b_i}\} + \Im\{\bar{x}_{a_i}\}\Im\{\bar{x}_{b_i}\} \right), \tag{20b}$$

$$\mathbf{I}_{2,3} = \mathbf{I}_{3,2} = -\mathbf{I}_{1,4} = -\mathbf{I}_{4,1} = \frac{2}{\sigma^2} \sum_{i=1}^{N} \left(\Re\{\bar{x}_{b_i}\}\Im\{\bar{x}_{a_i}\} - \Re\{\bar{x}_{a_i}\}\Im\{\bar{x}_{b_i}\} \right). \tag{20c}$$

Proof: See Appendix E. ■

EM - Complexity per iteration		
(Eq. No.)	Additions	Multiplications
(12)	$3M+2$	$6M+6$
(11)	$NM(3M+4)$	$NM(6M+9)+5$
(13)	$4NM(3M+2)+3N+14$	$4NM(6M+8)+3N+33$
$\hat{h}_{ba}$	$15NM^2+12NM+3N+3M+16$	$30NM^2+41NM+3N+6M+44$
MMSE		
(17a)	$2N+1$	$2N+3$
(17b)	$2N+2$	$2N+3$
(17c)	$2N^2+N$	$5N^2+1$
(17d)	$N+1$	N
(16)	$M^N(2N^2+7N+5)$	$M^N(5N^2+6N+14)+2$
$\hat{h}_{ba}$	$M^N(6N^2+13N+8)+N+1$	$M^N(15N^2+10N+30)+N+4$

TABLE I: Complexity analysis of the estimators.

2) Data-aided BCRLB: Similarly, we derive the BCRLB for data-aided estimation, which is used as a benchmark for the MMSE estimator. The main result is presented in the proposition below.

Proposition 5: The *BCRLB* for estimation of parameters of interest is

$$\mathbf{var}(\hat{\boldsymbol{\phi}}_l) \geq \left[\left(\mathbb{E}_{\boldsymbol{\phi}}\left[\mathbf{I}(\boldsymbol{\phi})\right]+\mathbf{I}_4\right)^{-1}\right]_{l,l}, \tag{21}$$

where $l=\{1,2,3,4\}$, $\mathbf{I}_4$ is the 4×4 identity matrix and $\mathbb{E}_{\boldsymbol{\phi}}\left[\mathbf{I}(\boldsymbol{\phi})\right]=\mathbf{I}(\boldsymbol{\phi})$ and is given by equations (20b)- (20c) above.

Proof: See Appendix E. ■

D. Complexity Analysis

To evaluate the feasibility in implementing the proposed estimators, we investigate the computational complexity of the estimators in terms of required floating point multiplications and additions (flops) [34].

Table I shows the number of multiplications and additions needed for both the EM and MMSE estimators for h_{ba}. Although we only present the complexity analysis of h_{ba}, a very similar complexity can also be observed for estimators of h_{aa}. In each row of the table, the number of required additions and multiplications to implement a given equation is presented and are then summed to obtain overall complexity. It is clear from Table I, that the complexity of EM estimator, in terms of the big $\mathcal{O}$ notation, is $\mathcal{O}(n_{itr}NM^2)$ where n_{itr} denotes average number of iterations required for the EM algorithm to converge. On the other hand, the complexity of MMSE estimator is $\mathcal{O}(M^N)$ and grows exponentially

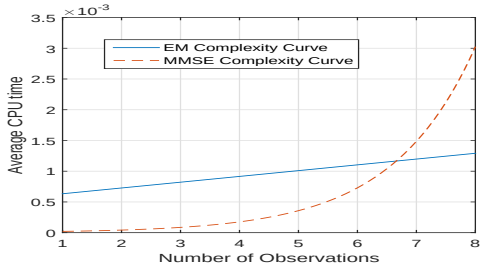

Fig. 5: The average CPU time vs. number of observations for $M = 2$ and SNR = 20 dB.

TABLE II: Average CPU time for different numbers of observations.

EM estimator		MMSE estimator	
N	Average CPU Time (sec)	N	Average CPU Time (sec)
8	0.0012	8	0.0048
12	0.0016	12	0.0516
13	0.0016	13	0.1062
16	0.0020	16	0.8958

with the number of observations, and constellation size. As a check on the analysis presented in Table I, we provide numerical results on average CPU time for fixed modulation set, i.e., fixed M. We first provide individual average CPU time for each algorithm in Table II and then fit the curve to this data in Fig. 5 for more meaningful comparison.

Table II shows average CPU time over 100 channel realizations for different number of observations for MMSE and EM estimators when $M = 2$ at SNR = 20 dB. We use this data to plot average CPU time for the range of observations for both estimators in Fig. 5. The figure was obtained by the curve fitting toolbox of MATLAB. The fitting error was found to be 9.405×10^{-5} and 3.38×10^{-6} for the EM and the MMSE complexity plots, respectively. This figure confirms the earlier analysis in Table I where it was shown that the complexity of MMSE estimator grows exponentially with number of observations as opposed to linear growth of the EM algorithm. Consequently, after certain number of observations the EM estimator becomes more computationally efficient compared to the MMSE estimator. From Fig. 5 this number of observations is found to be $N > 6$, for BPSK modulation.

VI. Simulation Results

Simulation results are presented to illustrate the performance of the proposed estimators with modulation sets proposed in Section IV. Results for estimating h_{ba} are only provided since identical results are obtainable for h_{aa}. We define SNR $\triangleq \frac{\Delta}{\sigma^2}$, where Δ is the total average power and σ^2 is the noise variance. For each simulation run, N data and interfering symbols are randomly generated assuming uniform distribution for both. Noise and random channel realizations are also generated according to the models presented in Sections II and V, respectively. The figure of merit used is the average MSE, which is obtained by averaging over 1000 simulation runs. We first present the results for shifted modulation sets and investigate (i) the effect of shift on the MSE of the estimators, and (ii) the bit error rate (BER) for the shifted modulation set. We then investigate the performance of the proposed

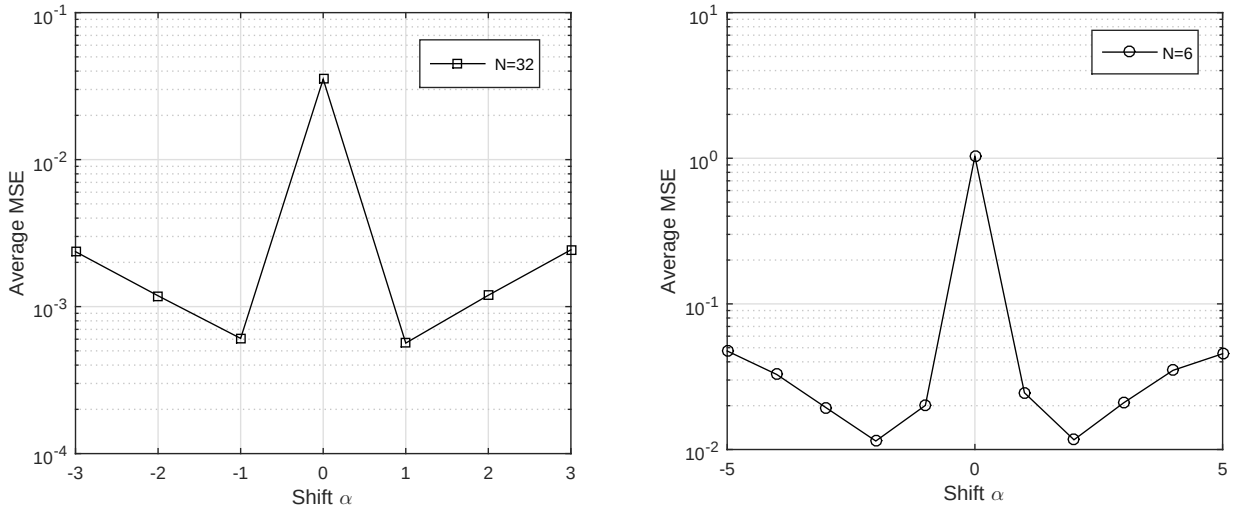

(a) EM estimator.

(b) MMSE estimator.

Fig. 6: Effect of shift in the modulation set on the average MSE performance with SNR = 20 dB and BPSK modulation.

estimators with a rotated modulation constellation. We conclude this section by investigating the effect of increasing power of the self-interference signal on the performance of the estimators.

A. Shifted modulation set

In this section we investigate the performance of a shifted modulation set as satisfied by Theorem 1. For the results reported in this section, we normalize the shifted modulation set symbols so the average power is unity after the shift, i.e., $\Delta = 1$.

1) Effect of shift on estimator performance: The average MSE performance of the proposed estimators directly depends on the mean of the modulation set as is evident from the derived bounds in Section V. In this subsection we therefore parameterize this shift as α in the average MSE performance results. We apply different shifts, α, to BPSK modulation at SNR = 20 dB. Figs. 6(a) and 6(b) show the average MSE versus the shift for the MMSE estimator with $N = 6$, and EM estimator with $N = 32$, respectively. The figures show that the lowest average MSE occurs at different shifts for the estimators, i.e., $\alpha = \pm 2$ and $\alpha = \pm 1$ for the MMSE and EM estimators, respectively. Since EM and MMSE estimators share no similarity in their structure, it is not surprising that their average MSE results also respond differently to modulation shift α.

It is important to note that the optimum shift power given by Figs. 6(a) and 6(b) for EM and MMSE estimators does not significantly change the peak-to-average-power ratio (PAPR) of the conventional

modulation sets. Consequently, symbols modulated by the proposed set will not exceed the dynamic range of power amplifiers.

Unless stated otherwise, throughout the remainder of this section we will use shifted modulation set with α determined via the investigation in Figs. 6(a) and 6(b).

2) Esimator performance:

a) EM Estimator: Performance of the EM estimator is investigated for different modulation sets and different numbers of observations.

MSE performance: In the derivation of the PDF in (4), a uniform probability mass function (PMF) was assumed for the elements of modulation set. With this assumption is expected that the frequency of the elements of modulation set in a given transmitted symbols are all the same. To ensure that this assumption is satisfied, the length of transmitted sequence should be greater than certain N. This number was empirically found to be $N > 32$ for the EM estimator. Therefore, for shifted BPSK modulation set with $\alpha = 1$, average MSE performance was obtained for $N = 32, 48$, as presented in Fig. 7(a). This figure shows that the EM estimator performance with shifted modulation set reaches the performance of the data-aided bound at high SNR. This is expected and can be explained intuitively by noting that the EM estimator tries to estimate the parameters of a Gaussian mixture distribution, while the data-aided bounds are representative of the best obtainable performance by pilot-based estimators. Pilot-based estimators estimate parameters of a Gaussian distribution. At high SNR, the mixture distribution converges to Gaussian distribution as one dominant component in the mixture emerges. *BER performance*: We also investigate the BER performance of the overall FD system once the EM estimator is used for channel estimation, for shifted BPSK and QPSK modulation sets with $\alpha = 1$. These results are obtained with $N = 128$ observations used for channel estimation, and are presented in Fig. 7(b). The difference between the BER results of BPSK and QPSK modulation can be explained by noting that for a given transmit power, BER performance of BPSK is well-known to be superior. Consequently, each channel has less energy and the probability of false bit detection increases for QPSK modulation. On the same plot, we also compare the BER performance of BPSK and QPSK modulations with the proposed EM estimator, by the BER performance, when perfect channel state information (CSI) is available at the receiver. As shown in Fig. 7(b), the difference between the BER performance in the two cases, is very small, especially in the high SNR region. This can be explained by the fact that the estimator approaches the performance of its theoretical bound after a certain SNR, making channel estimation error becomes insignificant. Consequently, BER performance is not significantly degraded.

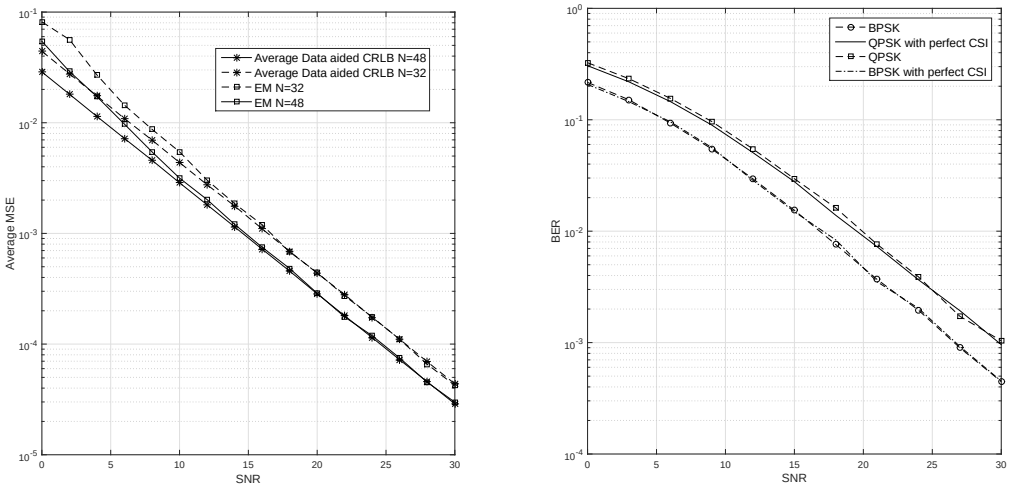

(a) Average MSE vs. SNR for different N when non-zero-mean BPSK modulation is used.

(b) BER performance for shifted BPSK and QPSK modulation for EM estimator.

Fig. 7: Performance analysis for EM-based estimator with shifted modulation set.

b) MMSE Estimator: Performance is investigated for different numbers of observations. Despite the fact that the MMSE estimator is based on an assumed uniform PMF for modulated symbols, it was found to be less sensitive to this assumption compared to the EM estimator. Simulation of the MMSE estimator with the same number of observation as the EM estimator results in prohibitive complexity while providing no extra insights. In addition, we show in Section VI-C, that a maximum of $N = 16$ observations are sufficient for MMSE estimator. Hence, we preset MMSE results with lower numbers of observations.

MSE performance: Next, average MSE performance is compared to average BCRLB. To avoid the prohibitive computational complexity of the MMSE estimator, we only present average MSE results for $N = 6, 16$, and the shifted BPSK modulation set with $\alpha = 2$, in Fig. 8(a). Although the MMSE estimator is derived based on the assumption of uniformly distributed transmitted symbols, we note that the estimator performs well for small values of N, e.g., $N = 16$. Nevertheless, we note some degradation in performance for $N = 6$ as seen in Fig. 8(a).

BER performance: We also investigate BER of FD communication system with shifted BPSK modulation set with $\alpha = 2$, as shown in Fig. 8(b). The figure shows that the performance is within 1 to 2 dB of the ideal performance when perfect CSI is available.

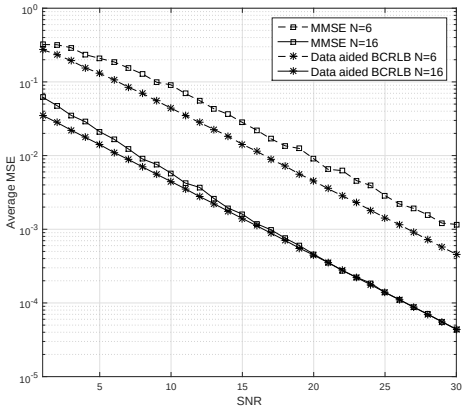

(a) Average MSE vs. SNR.

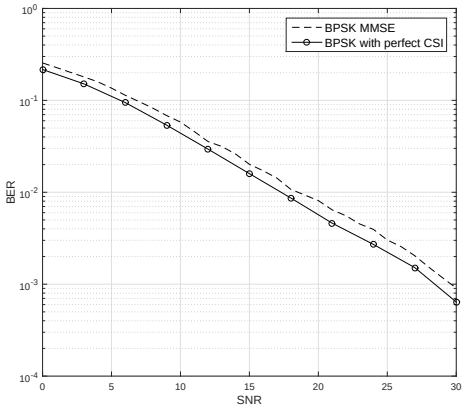

(b) BER vs. SNR.

Fig. 8: Performance analysis for MMSE estimator with shifted BPSK.

B. Rotated modulation set

Next, we investigate the performance of a rotated modulation set proposed in (7). We note that finding the optimum rotation for a rotated modulation set is not straightforward unlike finding an optimum shift for shifted modulation set, and is a subject of future investigation. However, we may still apply Theorem 1 to an asymmetric constellation by rotating zero-mean BPSK modulation set by $\psi_1 = 0$ and $\psi_2 = \frac{\pi}{4}$. The simulation parameters are otherwise kept the same as for the case of the shifted modulation set. Asymmetric rotation of the modulation constellation will also generate an asymmetric modulation constellation. Hence, the overall effect is similar to that of the shifted modulation set. To show this we only present the simulation results for the EM estimator. Fig. 9(a) shows the performance of the EM estimator for $N = 32, 48$. As expected, similar to the shifted modulation set the estimators reach the performance of the corresponding data-aided bounds. Fig. 9(b) shows the BER performance of the FD system with the proposed EM estimator for the rotated modulation constellation with $N = 128$. The BER performance is almost the same as the BER performance of a FD system with perfect CSI. This is due to the low channel estimation error observed in Fig. 9(a).

C. Required number of observations, N

It has been reported in [14] that FD systems outperform HD systems in terms of capacity once the channel MSE is less than 0.02. Hence, a value of N which can achieve MSE ≤ 0.02 with reasonable SNR is sufficient. Figs. 7(a), 9(a) show that the EM-based estimator can achieve MSE ≤ 0.02 with $N = 32$ for SNR ≥ 5 dB for the optimum shifted modulation set and SNR ≥ 10 dB with the simple

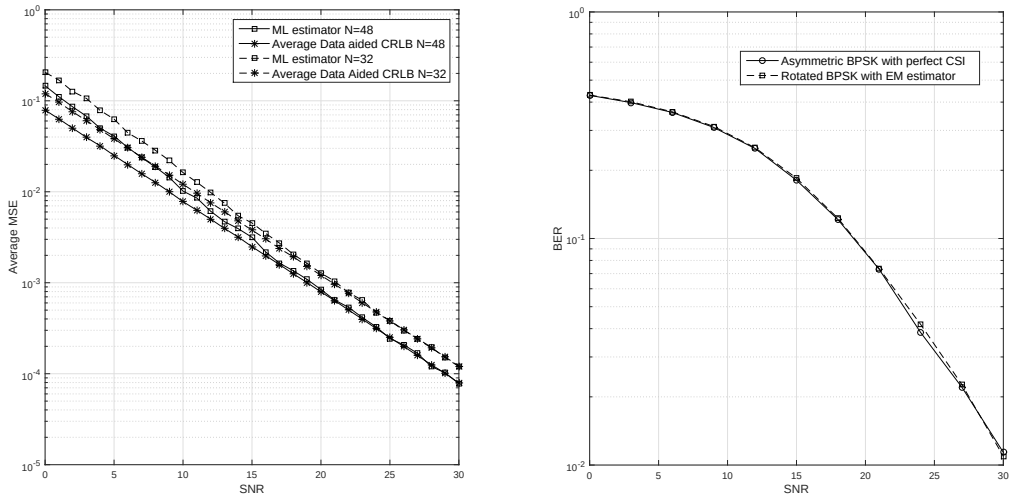

(a) Average MSE vs. SNR.

(b) BER vs. SNR.

Fig. 9: Performance analysis for EM estimator with rotated BPSK.

rotated BPSK modulation set. Figs. 8(a), again show that the MMSE based estimator can achieve MSE ≤ 0.02 with $N = 16$ for SNR ≥ 5 dB for the shifted modulation set and SNR ≥ 10 dB with the simple rotated BPSK modulation set.

For the same value of N, the MMSE estimator outperforms the EM estimator. However, as shown in Fig. 5, the complexity of MMSE estimation becomes increasingly significant, compared to EM for $N > 6$. This is why the same value of N is not used for the two estimators.

D. Effect of increasing power on the self-interference channel on estimator performance

Thus far, it has been assumed that both self-interference and communication channels have the same power. This assumption is justified by knowing that the most effective self-interference cancellation in FD communication is obtained when both analog and passive self-interference cancellation are deployed; without these cancelation stages the range of analogue to digital converter (ADC) saturates [3], [9]. Hence, the power of the interfering signal is significantly reduced before it reaches the baseband processor. In this subsection we show that the identifiability analysis and proposed estimators are valid for any self-interference power. With no passive or analog self-interference canceller the signal to interference ratio (SINR) could be as low as -100 dB [3], while by deploying passive cancellation, SINR could be enhanced to -50 dB [40]. The effect of this self-interference power variation on the performance of the estimators at SNR = 20 dB, while both noise and desired signal powers are held

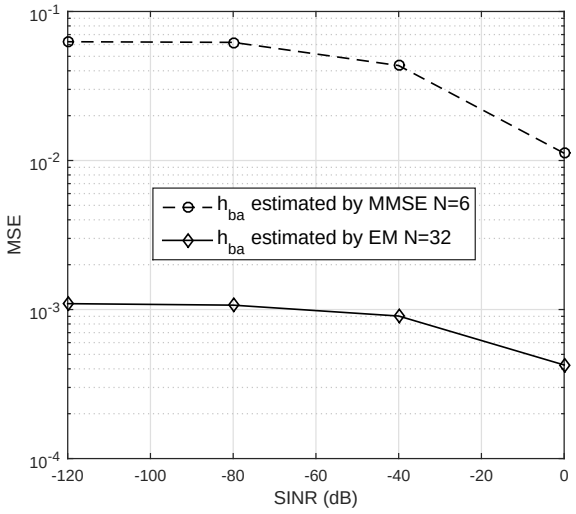

Fig. 10: Effect of self-interfering power on the channel estimation performance at SNR = 20 dB.

fixed is demonstrated. As expected, Fig. 10 shows that as the power of self-interfering signal increases, the performance of the estimators deteriorate. However, this performance degradation occurs at a very slow rate relative to the increasing self-interference power, which indicates robustness of the proposed estimators. This is not surprising since in FD communication the self-interference signal is completely known to the receiver [3]. Consequently, no matter how clean the self-interfering channel is, the effect on channel estimation is not significant. This is also evident from (4), where the exponent of the exponential function, i.e., $|y_{a_i} - h_{ba}x_k - h_{aa}x_{a_i}|^2$ can be approximated by $|h_{ba}x_{b_i} - h_{ba}x_k|^2$ at high SNRs, which is independent of h_{aa}. This shows that significant performance variation as a function of self-interference signal is not expected. The plot of Fig. 10 also highlights the effectiveness of the proposed estimators in that even with weak passive cancellation, i.e., SINR=120 dB, channel estimation error is not significant. This in turn means that effective self-interference cancellation is still possible with active cancellation.

VII. Conclusion

A new framework for blind ambiguity-free channel estimation in FD communication systems is developed that involves shifting or rotating modulation sets and avoids self-calibration, analog pilots, and bandwidth expansion. Based on these modulation sets, we have derived EM and MMSE estimators of the both self-interference and communication channels. The estimators are shown to asymptotically reach the performance of data aided bounds at high SNR. Our results have shown that the MMSE estimator, while requiring no initialization and few observations, has computational complexity that

increases exponentially in the number of observations and with constellation size. On the other hand, the EM estimator is found to be computationally efficient but it is sensitive to initialization. Simulations also show that the estimators can reach the performance of corresponding data-aided bounds when a rotated modulation set is used. In addition, simulation results reveal that the proposed estimators with asymmetric modulation sets are robust to increasing self-interference power. Future work may consider the application of the proposed framework for channel estimation in related system models found in relaying and interference limited networks.

APPENDIX A
PROOF OF LEMMA 1

Throughout this proof, we assume $k' \triangleq \Pi(k)$, $\forall k \in \mathcal{K}$, where $\Pi(\cdot)$ is a one-to-one and onto function on $\mathcal{K} \rightarrow \mathcal{K}$, and denote the symbols from the modulation set $\mathcal{A}$ and permuted modulation set $\mathcal{A}'$ by x_k and $x_{k'}$, respectively. We proceed with the proof of Lemma 1, by defining,

$$f(\mathbf{y_a}, x_k; \boldsymbol{\theta}) \triangleq \left(\frac{1}{M\pi\sigma^2}\right)^N \prod_{i=1}^{N} \sum_{k=1}^{M} \underbrace{\exp\left(\frac{-1}{\sigma^2}|y_{a_i} - \boldsymbol{\theta}(1)x_{a_i} - \boldsymbol{\theta}(2)x_k|^2\right)}_{\triangleq f_k(y_{a_i}, \boldsymbol{\theta})}, \tag{A.1a}$$

$$f(\mathbf{y_a}, x_{k'}; \boldsymbol{\theta}') \triangleq \left(\frac{1}{M\pi\sigma^2}\right)^N \prod_{i=1}^{N} \sum_{k'=1}^{M} \underbrace{\exp\left(\frac{-1}{\sigma^2}|y_{a_i} - \boldsymbol{\theta}'(1)x_{a_i} - \boldsymbol{\theta}'(2)x_{k'}|^2\right)}_{\triangleq f_{k'}(y_{a_i}, \boldsymbol{\theta}')}. \tag{A.1b}$$

where $\boldsymbol{\theta}(1)$, $\boldsymbol{\theta}(2)$, and $\boldsymbol{\theta}'(1)$, $\boldsymbol{\theta}'(2)$ represent the first and second elements of $\boldsymbol{\theta}$ and $\boldsymbol{\theta}'$, respectively. From (A.1a) and (A.1b), it is easy to see that if a permuted set $\mathcal{A}'$ exists such that $\frac{x_k}{x_{k'}}$ is constant $\forall k$, then $f(\mathbf{y_a}, x_k; \boldsymbol{\theta}) = f(\mathbf{y_a}, x_{k'}; \boldsymbol{\theta}')$ for $\boldsymbol{\theta} \neq \boldsymbol{\theta}'$. This is because for $\boldsymbol{\theta}'(1) = \boldsymbol{\theta}(1)$ and $\boldsymbol{\theta}'(2) = \frac{\boldsymbol{\theta}(2)x_k}{x_{k'}}$, i.e., $\boldsymbol{\theta}' = [\boldsymbol{\theta}(1), \frac{\boldsymbol{\theta}(2)x_k}{x_{k'}}]$, $f(\mathbf{y_a}, x_k; \boldsymbol{\theta}) = f(\mathbf{y_a}, x_{k'}; \boldsymbol{\theta}')$.

However, to complete the proof we also need to show that if we have an identifiability problem then a permuted set $\mathcal{A}'$ exists such that $\frac{x_k}{x_{k'}}$ is constant. In other words if $f(\mathbf{y_a}; \boldsymbol{\theta}) = f(\mathbf{y_a}; \boldsymbol{\theta}')$, for $\boldsymbol{\theta} \neq \boldsymbol{\theta}'$, then there must exist a $\mathcal{A}'$ such that $\frac{x_k}{x_{k'}}$ is constant.

It is an elementary fact from probability theory that if two joint densities are equal over the same probability space, then their corresponding marginal densities are equal [41]. Therefore, if $f(\mathbf{y}_a; \boldsymbol{\theta}) = f(\mathbf{y}_a; \boldsymbol{\theta}')$ $\forall i$, then

$$\sum_{k=1}^{M} f_k(y_{a_i}, x_k; \boldsymbol{\theta}) = \sum_{k'=1}^{M} f_{k'}(y_{a_i}, x_{k'}; \boldsymbol{\theta}'). \tag{A.2}$$

$\forall i$. We note that the transmit symbols are uniformly distributed, i.e, $P(x_k) = \frac{1}{M}$ $\forall i \in \mathcal{I}$, hence, we can conclude that if (A.2) holds, then

$$\sum_{k=1}^{M} \frac{f_k(y_{a_i}|x_k;\boldsymbol{\theta})P(x_k)}{f(y_{a_i})} = \sum_{k'=1}^{M} \frac{f_{k'}(y_{a_i}|x_{k'};\boldsymbol{\theta}')P(x_{k'})}{f(y_{a_i})}. \tag{A.3}$$

Cancelling terms of (A.3) we have

$$\sum_{k=1}^{M} f_k(y_{a_i}|x_k;\boldsymbol{\theta}) = \sum_{k'=1}^{M} f_{k'}(y_{a_i}|x_{k'};\boldsymbol{\theta}'). \tag{A.4}$$

Finally, if (A.4) holds, then

$$f_k(y_{a_i}|x_k;\boldsymbol{\theta}) = f_{k'}(y_{a_i}|x_{k'};\boldsymbol{\theta}'), \tag{A.5}$$

for $k \in \mathcal{K}$.

Case I: We first assume that the interfering symbols are not all the same, i.e., x_{a_i} is different for $\forall i \in \mathcal{I}$, as this does not happen in reality. There are three different possible $\boldsymbol{\theta}'$, i.e., (i) $\boldsymbol{\theta}' = [h_{aa}, h'_{ba}]$, (ii) $\boldsymbol{\theta}' = [h'_{aa}, h_{ba}]$ and (iii) $\boldsymbol{\theta}' = [h'_{aa}, h'_{ba}]$, corresponding to the cases where either the first or the second element or both elements of $\boldsymbol{\theta}$ are different. Consequently, (A.5) can only hold with these possible $\boldsymbol{\theta}'$

1) If $\boldsymbol{\theta}' = [h_{aa}, h'_{ba}]$ and if (A.5) holds $\forall k$ then

$$\exp\left(\frac{-1}{\sigma^2}|y_{a_i} - h_{aa}x_{a_i} - h_{ba}x_k|^2\right) = \exp\left(\frac{-1}{\sigma^2}|y_{a_i} - h_{aa}x_{a_i} - h'_{ba}x_{k'}|^2\right), \tag{A.6}$$

$\forall k$. Via some algebraic manipulations and rearranging, it can be shown that if (A.6) holds, $\forall k$, then

$$\frac{x_k}{x_{k'}} = \frac{h'_{ba}}{h_{ba}}, \tag{A.7}$$

$\forall k$. We note that the right hand side of (A.7) is independent of k, and hence, is constant. For left hand side to be a constant there should exist a permuted set $\mathcal{A}'$ such that $\frac{x_k}{x_{k'}}$ is constant $\forall k$.

2) If $\boldsymbol{\theta}' = [h'_{aa}, h_{ba}]$ and (A.5) holds, then following the approach taken above, it can be easily shown that

$$\frac{h_{ba}(x_k - x_{k'})}{x_{a_i}} + h_{aa} = h'_{aa}. \tag{A.8}$$

While the right hand side of (A.8) is constant $\forall i$, the left hand side varies because of the term x_{a_i}. However, we started with the assumption that x_{a_i} is not constant $\forall i$. Consequently, the left hand side of (A.8) will never be a constant and (A.5) does not hold $\forall k$ with this $\boldsymbol{\theta}'$, regardless of the permuted set $\mathcal{A}'$.

3) If $\boldsymbol{\theta}' = [h'_{aa}, h'_{ba}]$ and (A.5) holds, then following the approach taken in the previous two scenarios, it is easy to show that the un-identifiability of $\boldsymbol{\theta}$ depends on constant transmitted symbols, and

because the transmitted symbols are not same, in this scenario again (A.5) does not hold $\forall k$ with this $\boldsymbol{\theta}'$.

The above analysis shows that assuming transmitted symbols are not the same and if we have identifiability problem then a permuted set $\mathcal{A}'$ should exist such that $\frac{x_k}{x_{\Pi(k)}}$ is constant $\forall k$. If such a permuted set exist then $f(\mathbf{y}_a;\boldsymbol{\theta}) = f(\mathbf{y}_a;\boldsymbol{\theta}')$ and $\boldsymbol{\theta}' = [h_{aa}, h'_{ba}]$.

Case II: In the case of same symbols being transmitted, following the same argument as the previous case where the transmitted symbols were assumed distinct, (A.5) should be checked for the following scenarios: (i) $\boldsymbol{\theta}' = [h_{aa}, h'_{ba}]$, (ii) $\boldsymbol{\theta}' = [h'_{aa}, h_{ba}]$ and (iii) $\boldsymbol{\theta}' = [h'_{aa}, h'_{ba}]$.

1) If $\boldsymbol{\theta}' = [h_{aa}, h'_{ba}]$ and (A.5) holds $\forall k$, then it is clear that there should exist a permuted set $\mathcal{A}'$ such that $\frac{x_k}{x_{k'}}$ is constant, regardless of the same symbols being transmitted or not.
2) If $\boldsymbol{\theta}' = [h'_{aa}, h_{ba}]$ and (A.5) holds $\forall k$, then (A.8), which depends on x_{a_i}, should hold true. Hence, there should exist a permutation $\Pi(\cdot)$ for which $x_k - x_{\Pi(k)} = c$ is constant $\forall k$. It can be shown that the permutation function that satisfies this condition is an involution [26],i.e., $\Pi() = \Pi^{-1}()$. This in turn means, $x_k - x_{\Pi(k)} = x_{\Pi(k)} - x_k$ or $x_k = x_{\Pi(K)}$ which corresponds to no permutation. Consequently, (A.5) cannot hold $\forall k$ with this $\boldsymbol{\theta}'$.
3) If $\boldsymbol{\theta}' = [h'_{aa}, h'_{ba}]$ and (A.5) holds $\forall k$, then in a similar fashion to the previous scenario it can be shown that given the constellation diagram of zero-mean modulation sets, (A.5) cannot hold $\forall k$ with this $\boldsymbol{\theta}'$. We omit the detailed analysis for space considerations.

Consequently, in both cases, if we have an identifiability problem then a permuted set $\mathcal{A}'$ should exist such that $\frac{x_k}{x_{\Pi(k)}}$ is constant $\forall k$ and if such a permuted set exist then $f(\mathbf{y}_a;\boldsymbol{\theta}) = f(\mathbf{y}_a;\boldsymbol{\theta}')$ and $\boldsymbol{\theta}' = [h_{aa}, h'_{ba}]$.

We proved if there exists a permuted set $\mathcal{A}'$ such that $\frac{x_k}{x_{\Pi(k)}}$ is constant $\forall k$, then we have identifiability problem. We also proved that if we have identifiability problem then a permuted set $\mathcal{A}'$ should exist such that $\frac{x_k}{x_{\Pi(k)}}$ is constant $\forall k$. Hence, we can conclude that $\boldsymbol{\theta}$ is not identifiable from (5), if and only if a permuted set $\mathcal{A}'$ exists, such that $\frac{x_k}{x_{\Pi(k)}}$ is a constant $\forall k \in \mathcal{K}$.

APPENDIX B
PROOF OF THEOREM 1

From Theorem 1 we know that if for a constant c there exists a one-to-one and onto function $\Pi(\cdot)$ on $\mathcal{K} \to \mathcal{K}$ for which,

$$\frac{x_1}{x_{\Pi(1)}} = \frac{x_2}{x_{\Pi(2)}} = \cdots = \frac{x_M}{x_{\Pi(M)}} = c, \tag{B.1}$$

then $\boldsymbol{\theta}$ is not identifiable from (4). Without loss of generality we assume $x_{\pi(k)} = x_{k'} \in \mathcal{A}$ then if $\frac{x_k}{x_{\Pi(k)}} = c \ \forall k$, we can conclude that $\frac{x_k}{x_{\Pi(k)}} = \frac{x_{k'}}{x_{\Pi(k')}} = c$ or $\frac{x_k}{x_{\Pi(k)}} = \frac{x_{\Pi(k)}}{x_{\Pi(k')}} = c$. However, we know that $\Pi(\cdot)$ is a one-to-one and onto function on $\mathcal{K} \to \mathcal{K}$. Hence, it can be shown that for this function to satisfy (B.1), then $\Pi^{-1}(\cdot) = \Pi(\cdot)$, i.e., involution [26]. Consequently, if $x_{\pi(k)} = x_{k'}$, then $x_{\pi(k')} = x_k$ and therefore $\frac{x_k}{x_{\Pi(k)}} = \frac{x_{\Pi(k)}}{x_k} = c$. For this reason the constant c can only be 1 or -1. However, for $c = 1$, $x_k = x_{\Pi(k)} \ \forall k$ which means no permutation. This means that θ is not identifiable according to Theorem 1 if there exists a one-to-one and onto function $\Pi(\cdot)$ for which, $x_k = -x_{\Pi(k)} \ \forall k$. Consequently, if $\forall k$, the reflection of x_k around the origin, i.e., $-x_k$ is in the modulation set $\mathcal{A}$, then θ is not identifiable. In other words, if the constellation diagram is asymmetric around the origin, then ambiguity-free blind estimation is possible.

APPENDIX C
PROOF OF PROPOSITION 1

In this appendix, the equations for the EM algorithms which are used to find the ML solution of (10) are derived. We assume both transmitters at nodes a and b use asymmetric modulation set $\bar{\mathcal{A}}$, i.e., $\bar{x}_{a_i}, \bar{x}_{b_i} \in \bar{\mathcal{A}}$, and assume a uniform discrete distribution for the transmitted symbols.

A. *Proof of E-Step*

In the E-step of the algorithm function $Q(\boldsymbol{\phi}; \boldsymbol{\phi}^{(n)})$ is given by

$$Q(\boldsymbol{\phi}|\boldsymbol{\phi}^{(n)}) = E_{\bar{\mathbf{x}}_b|\mathbf{y}_a;\boldsymbol{\phi}^{(n)}}[\ln f(\mathbf{y}_a, \bar{\mathbf{x}}_b|\boldsymbol{\phi})]. \tag{C.1}$$

To calculate (C.1), we require $\ln f(\mathbf{y}_a, \bar{\mathbf{x}}_b|\boldsymbol{\phi})$. Hence, we start by the joint PDF

$$f(y_{a_i}, \bar{x}_{b_i}; \boldsymbol{\phi}) = f(y_{a_i}|\bar{x}_{b_i}; \boldsymbol{\phi}) P(\bar{x}_{b_i}) = \frac{1}{M\pi\sigma^2} \sum_{k=1}^{M} \mathbb{I}_{\{\bar{x}_k\}}(\bar{x}_{b_i}) \exp\left(\frac{-1}{\sigma^2}|y_{a_i} - h_{ba}\bar{x}_k - h_{aa}\bar{x}_{a_i}|^2\right), \tag{C.2}$$

where, $\mathbb{I}_{\{\bar{x}_k\}}(\bar{x}_{b_i}) = 1$ if $\bar{x}_k = \bar{x}_{b_i}$ and 0 otherwise. Consequently, the log-likelihood of all the observations is given by

$$\begin{aligned} \ln(f(\mathbf{y}_a, \mathbf{x}_b; \boldsymbol{\phi})) &= \sum_{i=1}^{N} \ln(f(y_{a_i}, \bar{x}_{b_i}; \boldsymbol{\phi})) \\ &= -N\ln(M\pi\sigma^2) - \frac{1}{\sigma^2} \sum_{i=1}^{N} \sum_{k=1}^{M} \mathbb{I}_{\{\bar{x}_k\}}(\bar{x}_{b_i}) |y_{a_i} - h_{ba}\bar{x}_k - h_{aa}\bar{x}_{a_i}|^2. \end{aligned} \tag{C.3}$$

The expectation in (C.1) is conditioned on knowing $\boldsymbol{\phi}^{(n)}$ during the nth iteration of the algorithm. $\boldsymbol{\phi}^{(n)}$ from the M-step provides the channel estimates $\hat{h}_{aa}$ and $\hat{h}_{ba}$ to the E-step. Hence, substituting (C.3) and the channel estimates in (C.1), we have

$$\begin{aligned} Q(\boldsymbol{\phi}|\boldsymbol{\phi}^{(n)}) &= E_{\bar{\mathbf{x}}_b|\mathbf{y}_a;\boldsymbol{\phi}^{(n)}}[\log f(\mathbf{y}_a, \bar{\mathbf{x}}_b; \boldsymbol{\phi})] \\ &= -N\ln(M\pi\sigma^2) - \frac{1}{\sigma^2}\sum_{i=1}^{N}\sum_{k=1}^{M} E_{\bar{\mathbf{x}}_b|\mathbf{y}_a;\boldsymbol{\phi}^{(n)}}[\mathbb{I}_{\{\bar{x}_k\}}(\bar{x}_{b_i})]|y_{a_i} - \hat{h}_{ba}\bar{x}_k - \hat{h}_{aa}\bar{x}_{a_i}|^2. \end{aligned} \tag{C.4}$$

Let us define a new function

$$T_{k,i}^{(n)} \triangleq E_{\bar{\mathbf{x}}_b|\mathbf{y}_a;\boldsymbol{\phi}^{(n)}}[\mathbb{I}_{\{\bar{x}_k\}}(\bar{x}_{b_i})]. \tag{C.5}$$

It should be noted that $T_{k,i}^{(n)}$ is zero for all values of $\bar{x}_{b_i}$ except for $\bar{x}_{b_i} = \bar{x}_k$. Therefore, $T_{k,i}^{(n)} = P(\bar{x}_{b_i} = \bar{x}_k|\mathbf{y}_a, \boldsymbol{\phi}^{(n)})$ and is given by:

$$T_{k,i}^{(n)} = P(\bar{x}_{b_i} = \bar{x}_k|\mathbf{y}_a, \boldsymbol{\phi}^{(n)}) = \frac{\exp\left(\frac{-1}{\sigma^2}|y_{a_i} - h_{ba}^{(n)}\bar{x}_k - h_{aa}^{(n)}\bar{x}_{a_i}|^2\right)}{\sum_{\bar{k}=1}^{M}\exp\left(\frac{-1}{\sigma^2}|y_{a_i} - \hat{h}_{ba}^{(n)}\bar{x}_{\bar{k}} - \hat{h}_{aa}^{(n)}\bar{x}_{a_i}|^2\right)}. \tag{C.6}$$

Finally, $Q(\boldsymbol{\phi}|\boldsymbol{\phi}^{(n)})$ can be found as in (11).

B. Proof of M-step

The maximization-step of the EM algorithm is given by

$$\boldsymbol{\phi}^{(n+1)} = \arg\max_{\boldsymbol{\phi}} Q(\boldsymbol{\phi}|\boldsymbol{\phi}^{(n)}) = \arg\min_{\boldsymbol{\phi}} \sum_{i=1}^{N}\sum_{k=1}^{M} T_{k,i}^{(n)}|y_{a_i} - \hat{h}_{ba}^{(n)}\bar{x}_k - \hat{h}_{aa}^{(n)}\bar{x}_{a_i}|^2. \tag{C.7}$$

Note that (C.7) is equivalent to maximizing (4).

If we define the following function

$$g(\boldsymbol{\phi}) \triangleq \sum_{i=1}^{N}\sum_{k=1}^{M} T_{k,i}^{(n)}|y_{a_i} - h_{ba}\bar{x}_k - h_{aa}\bar{x}_{a_i}|^2, \tag{C.8}$$

We can solve (C.7) for a local minimum, if and only if the Jacobian is zero, i.e., $\boldsymbol{J} = \mathbf{J}(g)(\boldsymbol{\phi}) = \mathbf{0}$, and the Hessian, i.e., $\boldsymbol{H} = \mathbf{H}(g)(\boldsymbol{\phi})$, is positive semi-definite. We define

$$\boldsymbol{S} \triangleq \begin{bmatrix} s_1 & 0 & s_2 & s_3 \\ 0 & s_1 & -s_3 & s_2 \\ s_2 & -s_3 & s_4 & 0 \\ s_3 & s_2 & 0 & s_4 \end{bmatrix}, \quad \boldsymbol{v} \triangleq \begin{bmatrix} v_1 \\ v_2 \\ v_3 \\ v_4 \end{bmatrix}, \tag{C.9}$$

where the elements of $\boldsymbol{S}$ and $\boldsymbol{v}$ are found by taking the derivative of $g(\boldsymbol{\theta})$ with respect to the four parameters, and are given by (14a)- (14b). Then, by taking the second derivatives of $g(\boldsymbol{\phi})$ with respect

to all four parameters, we can show that $\boldsymbol{H} = 2\boldsymbol{S}$. According to Sylvester's criterion [42], $\boldsymbol{H}$ is positive semi-definite if and only if all the following are positive

$$s_1, \quad \det\left(\begin{bmatrix} s_1 & 0 \\ 0 & s_1 \end{bmatrix}\right), \quad \det\left(\begin{bmatrix} s_1 & 0 & s_2 \\ 0 & s_1 & -s_3 \\ s_2 & -s_3 & s_4 \end{bmatrix}\right), \quad \det(\boldsymbol{S}). \tag{C.10}$$

It can easily be shown that $\det(\boldsymbol{S}) = (s_1 s_4 - s_2^2 - s_2^2)^2$, and is always positive. According to (14a), s_1 is always positive, and it is clear that the second determinant is always positive. However, the positivity of the third determinant, i.e., $s_1 s_4 - s_2^2 - s_3^2$, directly depends on the initialization. This is evident from definitions in (14a)- (14b) and the derivation of function $T_{k,i}^{(n)}$ in (C.6), which is a function of $\hat{h}_{aa}^{(n)}$ and $\hat{h}_{ba}^{(n)}$, i.e., the estimates from the nth iteration. This analysis reiterates the significance of EM algorithm initialization. Without a correct initialization, EM might not converge to a local maximum, and will rather converge to a stationary point [43, Chap:3]. With the right initialization we can then focus on the first condition, i.e., $\boldsymbol{J} = 0$. We have four different parameters and we need to differentiate with respect to each other. The first condition can be expressed as follows:

$$\boldsymbol{S}\boldsymbol{\phi}^{(n+1)} = \boldsymbol{v}, \tag{C.11}$$

where in above, $\boldsymbol{\phi}^{(n+1)}$ is the solution to the M-step of the algorithm.

APPENDIX D
PROOF OF PROPOSITION 2

In this section we derive the MMSE estimators for both the interference and communication channels and we prove that they are given by (15a) and (15b), respectively. The MMSE estimator of the desired parameter h_{ba} is given by [25]

$$\mathbb{E}[h_{ba}|\mathbf{y_a}] = \int_{-\infty}^{\infty} h_{ba} f(h_{ba}|\mathbf{y_a}) dh_{ba}. \tag{D.1}$$

We start the proof by focusing on the following conditional PDF and Bayes rule

$$f(h_{ba}|\mathbf{y_a}) = \frac{f(\mathbf{y_a}|h_{ba}) f(h_{ba})}{f(\mathbf{y_a})}. \tag{D.2}$$

We proceed by writing the conditional PDF of a single observation

$$f(y_{a_i}|h_{ba}, h_{aa}, \bar{x}_{b_i}) = \frac{1}{M\pi\sigma^2} \exp\left(\frac{-1}{\sigma^2}|y_{a_i} - h_{ba}\bar{x}_{b_i} - h_{aa}\bar{x}_{a_i}|^2\right), \tag{D.3}$$

where $\bar{x}_{a_i}, \bar{x}_{b_i} \in \bar{\mathcal{A}}$, i.e., an asymmetric modulation set is used. Then the conditional PDF of all observations is written as

$$f(\mathbf{y}_a|h_{ba}, h_{aa}, \bar{x}_{b_1}, \bar{x}_{b_2}, \cdots, \bar{x}_{b_N}) = \left(\frac{1}{\pi\sigma^2}\right)^N \exp\left(\frac{-1}{\sigma^2}\sum_{i=1}^{N}|y_{a_i} - h_{ba}\bar{x}_{b_i} - h_{aa}\bar{x}_{a_i}|^2\right). \tag{D.4}$$

By averaging out $\bar{x}_{bi}$, $\forall i \in \mathcal{I}$, from $f(\mathbf{y}_a, \bar{x}_{b_1}, \bar{x}_{b_2}, \cdots, \bar{x}_{b_N}|h_{ba}, h_{aa})$,

$$\begin{aligned} f(\mathbf{y}_a|h_{ba}, h_{aa}) &= \sum_{k_N=1}^{M}\cdots\sum_{k_1=1}^{M} f(\mathbf{y}_a|h_{ba}, h_{aa}, \bar{x}_{k_1}, \bar{x}_{k_2}, \cdots, \bar{x}_{k_N}) f(\bar{\mathbf{x}}) \\ &= \left(\frac{1}{M\pi\sigma^2}\right)^N \sum_{k_N=1}^{M}\cdots\sum_{k_1=1}^{M}\exp\left(\frac{-1}{\sigma^2}\sum_{i=1}^{N}|y_{a_i} - h_{ba}\bar{x}_{k_i} - h_{aa}\bar{x}_{a_i}|^2\right). \end{aligned} \tag{D.5}$$

Consequently, $f(\mathbf{y}_a|h_{ba})$ is given by

$$\begin{aligned} f(\mathbf{y_a}|h_{ba}) &= \int_{\mathbb{C}} f(\mathbf{y_a}|h_{aa}, h_{ba}) f(h_{aa}) dh_{aa} \\ &= \left(\frac{1}{M\pi\sigma^2}\right)^N \frac{1}{\pi}\int_{\mathbb{C}}\exp(-|h_{aa}|^2)\sum_{k_N=1}^{M}\cdots\sum_{k_1=1}^{M}\exp\left(\frac{-1}{\sigma^2}\sum_{i=1}^{N}|y_{a_i} - h_{ba}\bar{x}_{k_i} - h_{aa}\bar{x}_{a_i}|^2\right) dh_{aa} \\ &= \left(\frac{1}{M\pi\sigma^2}\right)^N \frac{1}{\pi}\sum_{k_N=1}^{M}\cdots\sum_{k_1=1}^{M}\int_{\mathbb{C}}\exp\left(\frac{-1}{\sigma^2}\sum_{i=1}^{N}|y_{a_i} - h_{ba}\bar{x}_{k_i} - h_{aa}\bar{x}_{a_i}|^2 - |h_{aa}|^2\right) dh_{aa}. \end{aligned} \tag{D.6}$$

To perform the integration in (D.6), we take advantage of the fact that the total probability of a complex Gaussian random variable $y \sim \mathcal{CN}(\mu, \sigma^2)$, is unity, i.e.,

$$\int_{\mathbb{C}} \frac{1}{\pi\sigma^2}\exp\left(\frac{-1}{\sigma^2}|y-\mu|^2\right) dy = 1. \tag{D.7}$$

and we manipulate the exponent in (D.6) into the form in (D.7), i.e., complete the square. Details of the algebraic manipulations are omitted. This results in

$$f(\mathbf{y_a}|h_{ba}) = \frac{K\pi\sigma^2}{\omega}\sum_{k_N=1}^{M}\ldots\sum_{k_1=1}^{M}\exp\left(-\frac{1}{\sigma^2}\left(\lambda - \frac{|\gamma^*|^2}{\omega^*}\right)\right), \tag{D.8}$$

where in (D.8)

$$\lambda \triangleq \sum_{i=1}^{N}\left(|y_{a_i}|^2 + |h_{ba}\bar{x}_{k_i}|^2 - 2\Re[y_{a_i}^* h_{ba}\bar{x}_{k_i}]\right), \tag{D.9}$$

$$\omega \triangleq \sum_{i=1}^{N}\left(\sigma^2 + \sum_{i=1}^{N}|\bar{x}_{a_i}|^2\right), \tag{D.10}$$

$$\gamma \triangleq \sum_{i=1}^{N}(\bar{x}_{a_i}h_{ba}^*\bar{x}_{k_i}^* - y_{a_i}^*\bar{x}_{a_i}). \tag{D.11}$$

The unconditional PDF $f(\mathbf{y_a})$ in (D.2) can be similarly expressed as

$$f(\mathbf{y_a}) = \int_{\mathbb{C}} f(\mathbf{y_a}|h_{ba}) f(h_{ba}) = \int_{\mathbb{C}} \frac{K\sigma^2}{\omega}\sum_{k_N=1}^{M}\ldots\sum_{k_1=1}^{M}\exp\left(-\frac{1}{\sigma^2}\left(\lambda - \frac{|\gamma^*|^2}{\omega^*} - |h_{ba}|^2\right)\right). \tag{D.12}$$

Similar to the previous approach for integrating (D.6), the integration in (D.12) is carried out by manipulating the exponent. Consequently, we arrive at (16). Finally, knowing (D.8) and (D.12) and by the application of Bayes rule, (15a) and (15b) are found.

APPENDIX E
PROOFS OF BOUNDS

A. CRLB Bound

For $l \in \{1,2,3,4\}$, the *CRLB* is [25]:

$$\mathbf{var}(\hat{\boldsymbol{\phi}}_l) \geq \left[\mathbf{I^{-1}}(\boldsymbol{\phi})\right]_{l,l}, \tag{E.1}$$

where in (E.1), $I(\boldsymbol{\phi})$ is the the Fisher information matrix (*FIM*), which for $l, l' \in \{1,2,3,4\}$ is given by [25]:

$$\mathbf{I}_{l,l'} = -\mathbb{E}_{\mathbf{y}_a}\left[\frac{\partial^2}{\partial_{\phi_m}\partial_{\phi_n}} \ln f(\mathbf{y}_a; h_{aa}, h_{ba})\right]. \tag{E.2}$$

If pilots are sent from an asymmetric modulation set $\bar{\mathcal{A}}$, then both $\bar{\mathbf{x}}_a$ and $\bar{\mathbf{x}}_b$ in (1) are known, consequently we can rewrite the system model as follows:

$$\mathbf{y}_a = [\bar{\mathbf{x}}_a, \bar{\mathbf{x}}_b]\begin{bmatrix} h_{aa} \\ h_{ba} \end{bmatrix} + \mathbf{w}_a. \tag{E.3}$$

For the system model in (E.3), the joint PDF of all observations is given by

$$f(\mathbf{y}_a; h_{aa}, h_{ba}) = \left(\frac{1}{\pi\sigma^2}\right)^N \exp \sum_{i=1}^{N}\left(\frac{-|y_{a_i} - h_{aa}\bar{x}_{a_i} - h_{ba}\bar{x}_{b_i}|^2}{\sigma^2}\right). \tag{E.4}$$

By evaluating (E.2), using the new joint PDF given by (E.4), the non-zero elements of $\mathbf{I}(\boldsymbol{\phi})$ can be found and are given by (20b)- (20c).

B. BCRLB Bound

The Bayesian information matrix (*BIM*) for a vector parameter $\boldsymbol{\phi}$ with prior information matrix *PIM* is given by [44]:

$$\textit{BIM} = \mathbb{E}_{\boldsymbol{\phi}}\left[\mathbf{I}(\boldsymbol{\phi})\right] + \textit{PIM}, \tag{E.5}$$

where in (E.5), $\mathbf{I}(\boldsymbol{\phi})$ is given by (20b)-(20c) and since all the elements of $\mathbf{I}(\boldsymbol{\phi})$ are independent of $\boldsymbol{\phi}$, $\mathbb{E}_{\boldsymbol{\phi}}\left[\mathbf{I}(\boldsymbol{\phi})\right] = \mathbf{I}(\boldsymbol{\phi})$. Finally, for $l, l' \in \{1,2,3,4\}$, *PIM* is defined as [44]

$$[\textit{PIM}]_{l,l'} = -\mathbb{E}_{\boldsymbol{\phi}}\left[\frac{\partial^2}{\partial_{\phi_l}\partial_{\phi'_l}} \ln f(\boldsymbol{\phi})\right]. \tag{E.6}$$

From the definition of the $\mathbf{\Phi}$ in (9), the prior distribution of each element of $\mathbf{\Phi}$ is known, i.e., $\Phi_l \sim \mathcal{N}(0, \frac{1}{2})$ for $l = \{1, 2, 3, 4\}$. Then, it can easily be shown that the off diagonal elements of *PIM* are all zero and the diagonal elements are given by:

$$[\mathit{PIM}]_{l,l} = \frac{1}{2}\mathbb{E}_{\boldsymbol{\phi}}[2] = 1. \tag{E.7}$$

Consequently, the *BCRLB* is given by (21).

REFERENCES

[1] A. Koohian, H. Mehrpouyan, M. Ahmadian, and M. Azarbad, "Bandwidth efficient channel estimation for full duplex communication systems," in *Proc. IEEE ICC*, Jun. 2015, pp. 4710–4714.

[2] Z. Zhang, X. Chai, K. Long, A. V. Vasilakos, and L. Hanzo, "Full duplex techniques for 5G networks: self-interference cancellation, protocol design, and relay selection," *IEEE Commun. Mag.*, vol. 53, no. 5, pp. 128–137, May 2015.

[3] A. Sabharwal, P. Schniter, D. Guo, D. W. Bliss, S. Rangarajan, and R. Wichman, "In-band full-duplex wireless: challenges and opportunities," *IEEE J. Sel. Areas Commun.*, vol. 32, no. 9, pp. 1637–1652, Sep. 2014.

[4] S. Hong, J. Brand, J. Choi, M. Jain, J. Mehlman, S. Katti, and P. Levis, "Applications of self-interference cancellation in 5G and beyond," *IEEE Commun. Mag.*, vol. 52, no. 2, pp. 114–121, Feb. 2014.

[5] E. Ahmed, A. Eltawil, and A. Sabharwal, "Rate gain region and design tradeoffs for full-duplex wireless communications," *IEEE Trans. Wireless Commun.*, vol. 12, no. 7, pp. 3556–3565, Jul. 2013.

[6] A. C. Cirik, Y. Rong, and Y. Hua, "Achievable rates of full-duplex MIMO radios in fast fading channels with imperfect channel estimation," *IEEE Trans. Signal Process.*, vol. 62, no. 15, pp. 3874–3886, Aug. 2014.

[7] Z. He, S. Shao, Y. Shen, C. Qing, and Y. Tang, "Performance analysis of RF self-interference cancellation in full-duplex wireless communications," *IEEE Wireless Communication Letters*, vol. 3, no. 4, pp. 405–408, Aug. 2014.

[8] W. Li, J. Lilleberg, and K. Rikkinen, "On rate region analysis of half- and full-duplex OFDM communication links," *IEEE J. Sel. Areas Commun.*, vol. 32, no. 9, pp. 1688–1698, Sep. 2014.

[9] M. Duarte, C. Dick, and A. Sabharwal, "Experiment-driven characterization of full-duplex wireless systems," *IEEE Trans. Wireless Commun.*, vol. 11, no. 12, pp. 4296–4307, Dec. 2012.

[10] D. Korpi, T. Riihonen, V. Syrjala, L. Anttila, M. Valkama, and R. Wichman, "Full-duplex transceiver system calculations: Analysis of ADC and linearity challenges," *IEEE Trans. Wireless Commun.*, vol. 13, no. 7, pp. 3821–3836, Jul. 2014.

[11] B. Kaufman, J. Lilleberg, and B. Aazhang, "An analog baseband approach for designing full-duplex radios," in *Proc. Asilomar Conf. on Signals, Syst. and Computers*, Nov. 2013, pp. 987–991.

[12] D. Korpi, L. Anttila, V. Syrjala, and M. Valkama, "Widely-linear digital self-interference cancellation in direct-conversion full duplex transceiver," *IEEE J. Sel. Areas Commun.*, vol. 32, no. 9, pp. 1674–1687, Sep. 2014.

[13] E. Everett, A. Sahai, and A. Sabharwal, "Passive self-interference suppression for full-duplex infrastructure nodes," *IEEE Trans. Wireless Commun.*, vol. 13, no. 2, pp. 680–694, Feb. 2014.

[14] D. Kim, H. Ju, S. Park, and D. Hong, "Effects of channel estimation error on full-duplex two-way networks," *IEEE Trans. Veh. Technol.*, vol. 62, no. 9, pp. 4666–4672, Nov. 2013.

[15] A. Masmoudi and T. Le-Ngoc, "A maximum-likelihood channel estimator for self-interference cancellation in full-duplex systems," *IEEE Trans. Veh. Technol.*, 2015 (to appear).

[16] J. Baltersee, G. Fock, and H. Meyr, "Achievable rate of mimo channels with data-aided channel estimation and perfect interleaving," vol. 19, no. 12, pp. 2358–2368, Dec 2001.

[17] E. Lehmann and G. Casella, *Theory of Point Estimation*. Springer Verlag, 1998.

[18] E. de Carvalho and D. T. M. Slock, "Blind and semi-blind FIR multichannel estimation: (global) identifiability conditions," *IEEE Trans. Signal Process.*, vol. 52, no. 4, pp. 1053–1064, Apr. 2004.

[19] L. Tong and S. Perreau, "Multichannel blind identification: from subspace to maximum likelihood methods," *in Proc. IEEE*, vol. 86, no. 10, pp. 1951–1968, Oct. 1998.

[20] K. Abed-Meraim, W. Qiu, and Y. Hua, "Blind system identification," *Proc. IEEE*, vol. 85, no. 8, pp. 1310–1322, Aug. 1997.

[21] S. Abdallah and I. N. Psaromiligkos, "EM-based semi-blind channel estimation in amplify-and-forward two-way relay networks," *IEEE Wire. Com. Letters*, vol. 2, no. 5, pp. 527–530, Oct. 2013.

[22] ——, "Blind channel estimation for amplify-and-forward two-way relay networks employing M-PSK modulation," *IEEE Trans. Signal Process.*, vol. 60, no. 7, pp. 3604–3615, Jul. 2012.

[23] S. Zhang, S.-C. Liew, and H. Wang, "Blind known interference cancellation," *IEEE J. Sel. Areas Commun.*, vol. 31, no. 8, pp. 1572–1582, Aug. 2013.

[24] Y. Zhu, D. Guo, and M. L. Honig, "A message-passing approach for joint channel estimation, interference mitigation, and decoding," *IEEE Trans. Wireless Commun.*, vol. 8, no. 12, pp. 6008–6018, Dec. 2009.

[25] S. M. Kay, *Fundamentals of Statistical Signal Processing: Estimation Theory*. Upper Saddle River, NJ, USA: Prentice-Hall, Inc., 1993.

[26] S. Shirali and C. Yogananda, *Number Theory*, ser. Echoes from Resonance. Universities Press, 2003.

[27] A. P. Dempster, N. M. Laird, and D. B. Rubin, "Maximum likelihood from incomplete data via the EM algorithm," *Journal of the Royal Statistical Society, Series B*, pp. 1–38, 1977.

[28] V. Melnykov and I. Melnykov, "Initializing the EM algorithm in Gaussian mixture models with an unknown number of components," *Comput. Stat. Data Analysis*, vol. 56, no. 6, pp. 1381–1395, Jun. 2012.

[29] C. Biernacki, G. Celeux, and G. Govaert, "Choosing starting values for the EM algorithm for getting the highest likelihood in multivariate Gaussian mixture models," *Comput. Stat. Data Analysis*, vol. 41, no. 3-4, pp. 561–575, Jan. 2003.

[30] H. Ju, D. Kim, H. V. Poor, and D. Hong, "Bi-directional beamforming and its capacity scaling in pairwise two-way communications," *IEEE Trans. Wireless Commun.*, vol. 11, no. 1, pp. 346–357, Jan. 2012.

[31] A. A. Nasir, H. Mehrpouyan, S. D. Blostein, S. Durrani, and R. A. Kennedy, "Timing and carrier synchronization with channel estimation in multi-relay cooperative networks," *IEEE Trans. Signal Process.*, vol. 60, no. 2, pp. 793–811, Feb. 2012.

[32] A. Scherb, V. Kuhn, and K.-D. Kammeyer, "Cramer-Rao lower bound for semiblind channel estimation with respect to coded and uncoded finite-alphabet signals," in *Proc. Asilomar Conf. on Signals, Syst. and Computers*, vol. 2, Nov. 2004, pp. 2193–2197.

[33] S. Abdallah and I. N. Psaromiligkos, "Exact Cramer Rao bounds for semiblind channel estimation in Amplify-and-Forward Two-Way Relay Networks employing square QAM," *IEEE Trans. Wireless Commun.*, vol. 13, no. 12, pp. 6955–6967, Dec. 2014.

[34] H. Mehrpouyan and S. D. Blostein, "Bounds and algorithms for multiple frequency offset estimation in cooperative networks," *IEEE Trans. Wireless Commun.*, vol. 10, no. 4, pp. 1300–1311, Apr. 2011.

[35] B. Farhang-Boroujeny, "Pilot-based channel identification: proposal for semi-blind identification of communication channels," *Electronics Letters*, vol. 31, no. 13, pp. 1044–1046, Jun 1995.

[36] J. K. Tugnait and X. Meng, "On superimposed training for channel estimation: performance analysis, training power allocation, and frame synchronization," vol. 54, no. 2, pp. 752–765, Feb 2006.

[37] A. G. Orozco-Lugo, M. M. Lara, and D. C. McLernon, "Channel estimation using implicit training," vol. 52, no. 1, pp. 240–254, Jan 2004.

[38] F. M. d. Campo, R. Cumplido, R. Perez-Andrade, and A. G. Orozco-Lugo, "Hybrid architecture for data-dependent superimposed training in digital receivers," in *Reconfigurable Computing and FPGAs, 2008. ReConFig '08. International Conference on*, Dec 2008, pp. 355–360.

[39] F. M. del Campo, R. Cumplido, R. Perez-Andrade, and A. G. Orozco-Lugo, "A system on a programmable chip architecture for data-dependent superimposed training channel estimation," *Int. J. Reconfig. Comp.*, vol. 2009, pp. 912 301:1–912 301:10, 2009.

[40] A. Masmoudi and T. Le-Ngoc, "A maximum-likelihood channel estimator in MIMO full-duplex systems," in *Proc. IEEE VTC-Fall*, Sep. 2014.

[41] S. M. Ross, *A First Course in Probability*. Pearson Prentice Hall, 2010.

[42] G. Strang, *Linear Algebra and its applications*. Harcourt Brace Jovanovich Publishers, 1988.

[43] G. McLachlan and T. Krishnan, *The EM algorithm and extensions*, 2nd ed., ser. Wiley Series in Probability and Statistics. Wiley, 2008.

[44] H. L. Van Trees, *Detection, Estimation, and Modulation Theory. Part II*. New York: Wiley-Interscience, 2002.